

Article

Synthesis and Crystal Structures of the Quaternary Zintl Phases $\text{RbNa}_8\text{Ga}_3\text{Pn}_6$ ($\text{Pn} = \text{P}, \text{As}$) and $\text{Na}_{10}\text{NbGaAs}_6$

Hua He, Chauntae Tyson, and Svilen Bobev *

Department of Chemistry and Biochemistry, University of Delaware, Newark, DE 19716, USA

* Author to whom correspondence should be addressed; E-Mail: bobev@udel.edu;
Tel.: +1-302-831-8720; Fax: +1-302-831-6335.

Received: 21 December 2011; in revised form: 27 March 2012 / Accepted: 31 March 2012 /
Published: 11 April 2012

Abstract: The new Zintl compounds $\text{RbNa}_8\text{Ga}_3\text{Pn}_6$ ($\text{Pn} = \text{P}, \text{As}$) and $\text{Na}_{10}\text{NbGaAs}_6$ have been synthesized from the corresponding elements at high temperatures. $\text{RbNa}_8\text{Ga}_3\text{P}_6$ and $\text{RbNa}_8\text{Ga}_3\text{As}_6$ crystallize with a novel structure type that features trigonal planar $[\text{Ga}_3\text{P}_6]^{9-}$ and $[\text{Ga}_3\text{As}_6]^{9-}$ motifs, which are isosteric with the 1,3,5-trioxanetrione (a cyclic trimer of carbon dioxide). $\text{Na}_{10}\text{NbGaAs}_6$, an unforeseen side product of the same reactions boasts a structure, which is based on NbAs_4 and GaAs_4 tetrahedra, condensed by sharing common edges into $[\text{NbGaAs}_6]^{10-}$ dimers. The bonding characteristics of both structures are discussed. All three compounds reported herein represent the first compounds found in the respective quaternary systems.

Keywords: arsenides; crystal structure; phosphides; Zintl phases

1. Introduction

In the past 10–15 years, intermetallic clathrates have attracted widespread interest, largely due to their demonstrated potential in thermoelectrics development [1–4]. Having successfully synthesized $\text{Rb}_{7.3}\text{Na}_{16}\text{Ga}_{20}\text{Si}_{116}$ and $\text{Cs}_8\text{Na}_{16}\text{Ga}_{21}\text{Si}_{115}$ —the first clathrate-II compounds with mixed Ga and Si [5], as well as the first arsenic-based clathrates of type-I $\text{Rb}_8\text{Zn}_{18}\text{As}_{28}$ and $\text{Cs}_8\text{Cd}_{18}\text{As}_{28}$ [6], we extended our attention to the $A\text{-Ga-Pn}$ systems (A = alkali metal or mixtures of alkali metals, Pn = pnictogen, *i.e.*, group 15 element). Our motivation here was the idea to produce gallium-phosphide and/or gallium-arsenide clathrates (in analogy with the well-known III-V semiconductors, which are isoelectronic with Si and Ge), but so far, all synthetic efforts have failed to provide any evidence for the possible

existence of such compounds. Instead, these experiments afforded a number of binary, ternary, and even quaternary compounds, some of which are with novel structures.

With this paper we detail the synthesis and the structural characterization of the new quaternary Zintl compounds $\text{RbNa}_8\text{Ga}_3\text{As}_6$ and $\text{RbNa}_8\text{Ga}_3\text{P}_6$, which are isoelectronic and isostructural. They crystallize with a novel orthorhombic structure type, featuring a somewhat unusual building block— $[\text{GaPn}_3]^{6-}$ trigonal planar units (isosteric with the borate BO_3^{3-} , as well as carbonate CO_3^{2-} anions), which are cyclically trimerized into $[\text{Ga}_3\text{Pn}_6]^{9-}$ (isosteric with the metaborate anion $\text{B}_3\text{O}_6^{3-}$, as well as the 1,3,5-trioxanetrione, a cyclic trimer of carbon dioxide). We note here that while the ternary *A-Tr-Pn* (*Tr* = triel *i.e.*, group 13 element) phase diagrams have already been extensively explored, and many *A-Tr-Pn* compounds have been reported [7–12], very little is known about the corresponding *A'-A''-Tr-Pn* systems, where *A'* and *A''* are two different alkali metals. The newly identified $\text{RbNa}_8\text{Ga}_3\text{As}_6$ and $\text{RbNa}_8\text{Ga}_3\text{P}_6$ (formally A_3TrPn_2) underscore the utility of mixtures of chemically and spatially dissimilar cations for the discovery of new compounds with novel structures. On this note, we point out that the prevailing motifs in the structures of most ternary *A-Tr-Pn* compounds are $[\text{TrPn}_4]^{9-}$ tetrahedra, either isolated or condensed in different fashions to form diverse polyanionic structures, e.g., ${}^1[\text{AlAs}_2]^{3-}$ and ${}^1[\text{Al}_2\text{As}_3]^{3-}$ chains in Na_3AlAs_2 [7] and $\text{K}_3\text{Al}_2\text{As}_3$ [8], respectively; ${}^2[\text{Al}_2\text{Sb}_3]^{2-}$ and ${}^2[\text{Ga}_3\text{As}_4]^{3-}$ layers in $\text{K}_2\text{Al}_2\text{Sb}_3$ [9] and $\text{K}_3\text{Ga}_3\text{As}_4$ [10], respectively; and 3-D framework in $\text{Na}_9\text{In}_3\text{Bi}_6$ structure [11]. Planar $[\text{Ga}_3\text{As}_6]^{9-}$, $[\text{Ga}_3\text{Sb}_6]^{9-}$ and $[\text{Ga}_3\text{Bi}_6]^{9-}$ units, analogous to the ones described herein are known only for $\text{K}_{20}(\text{Ga}_3\text{As}_6)_2\text{As}_{0.66}$ and $\text{K}_{20}(\text{Ga}_3\text{Sb}_6)_2\text{Sb}_{0.66}$ [12]; and $\text{K}_{20}(\text{Ga}_3\text{Bi}_6)_2\text{Bi}_{0.66}$ [11].

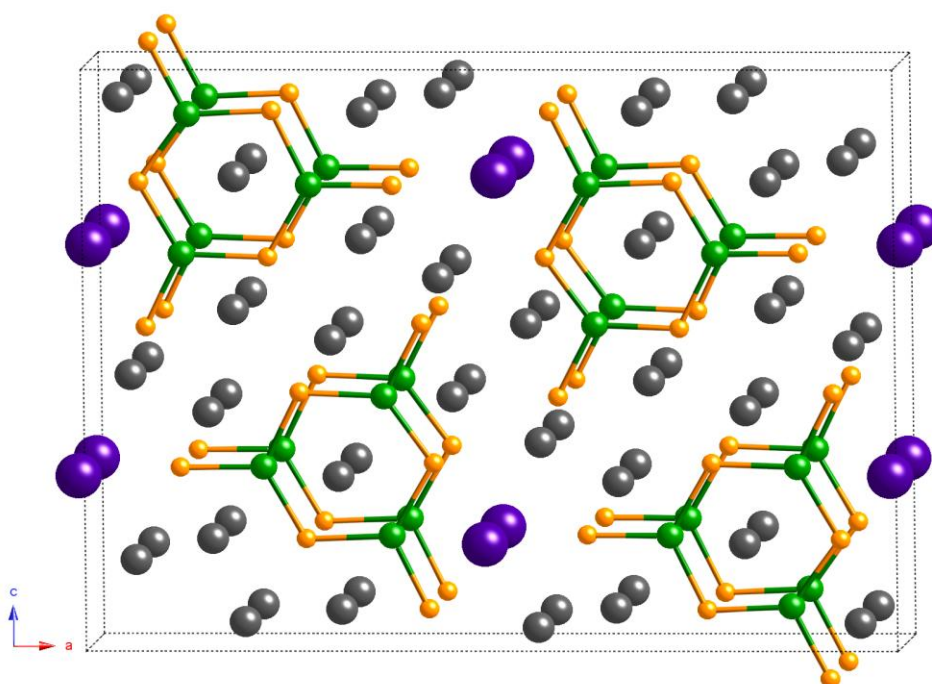
Reported as well is the new compound $\text{Na}_{10}\text{NbGaAs}_6$, which is isoelectronic and isostructural to $\text{K}_{10}\text{NbInAs}_6$ [13]. This phase was identified as an inadvertent product from the unwanted reaction of the reaction vessel (niobium) with elemental arsenic; its structure comprises NbAs_4 and GaAs_4 tetrahedra, edge-shared into $[\text{NbGaAs}_6]^{10-}$ dimers, which are isosteric with diborane molecule, B_2H_6 .

2. Results and Discussion

$\text{RbNa}_8\text{Ga}_3\text{As}_6$ and $\text{RbNa}_8\text{Ga}_3\text{P}_6$ both crystallize with the orthorhombic space group *Pnma* (No. 62, Pearson symbol *oP72*). The structure contains 18 independent sites in the asymmetric unit—one Rb, eight Na, three Ga, and six pnictogen atoms—all located at special position 4c. The structure can be viewed as being built from $[\text{Ga}_3\text{Pn}_6]^{9-}$ polyanions with alkali metal cations counterbalancing the charges and filling the space among them (Figure 1). The triangularly-shaped $[\text{Ga}_3\text{Pn}_6]^{9-}$ motif could be considered as a cyclic trimer of the $[\text{GaPn}_3]^{6-}$ trigonal planar units, which form a 6-membered ring by sharing two of the *Pn* atoms from each $[\text{GaPn}_3]^{6-}$. Therefore, all three Ga atoms are 3-bonded, while the three *Pn* atoms on the 6-membered ring are 2-bonded and the three *Pn* atoms attaching to the ring are 1-bonded. The distances between Ga and the *Pn* atoms are all within the normal ranges for covalently bound Ga–As and Ga–P. For example, the Ga–As distances range from 2.335 to 2.422 Å; the Ga–P distances range from 2.245 to 2.337 Å (Table 1). These values compare very well with the sums of the corresponding covalent radii ($r_{\text{Ga}} = 1.246$ Å; $r_{\text{As}} = 1.210$ Å; $r_{\text{P}} = 1.10$ Å) [14], as well as with the Ga–*Pn* distances found in compounds with Ga in similar 3-fold coordination environment of As or P (Table 2), e.g., $d_{\text{Ga-As}} = 2.367 \div 2.426$ Å in Rb_2GaAs_2 [15], $d_{\text{Ga-As}} = 2.367 \div 2.442$ Å in $\text{K}_{20}(\text{Ga}_3\text{As}_6)_2\text{As}_{0.66}$ [12], and $d_{\text{Ga-P}} = 2.226 \div 2.392$ Å in Rb_3GaP_2 [16]. In general, the distances

between Ga and the 2-bonded *Pn* are just about 0.08 Å longer than those between Ga and the 1-bonded *Pn* atom, which indicates that there is no appreciable π -bonding in the 6-membered ring. Hence, the formula $\text{RbNa}_8\text{Ga}_3\text{Pn}_6$ represents a salt-like, electron-balanced Zintl phase [17]. According to the valence rules, the charges could be assigned as $\text{Rb}^+(\text{Na}^+)_8(\text{Ga}^{3+})_3(\text{Pn}^{3-})_6$ based on oxidation states and counting the Ga and the *Pn* atoms as tri-valent species; alternatively, based on formal charges, the formula can be broken down to $\text{Rb}^+(\text{Na}^+)_8(3b\text{-Ga}^0)_3(2b\text{-Pn}^{1-})_3(1b\text{-Pn}^{2-})_3$, where 2-bonded and 1-bonded *Pn* atoms carry different negative charges, consistent with the Zintl formalism.

Figure 1. Crystal structure of $\text{RbNa}_8\text{Ga}_3\text{Pn}_6$ (*Pn* = P, As). The different elements are color-coded as follows: Ga—green; *Pn*—orange; Rb—purple; and Na—grey. The covalent Ga–*Pn* bonds are emphasized as yellow-green cylinders.



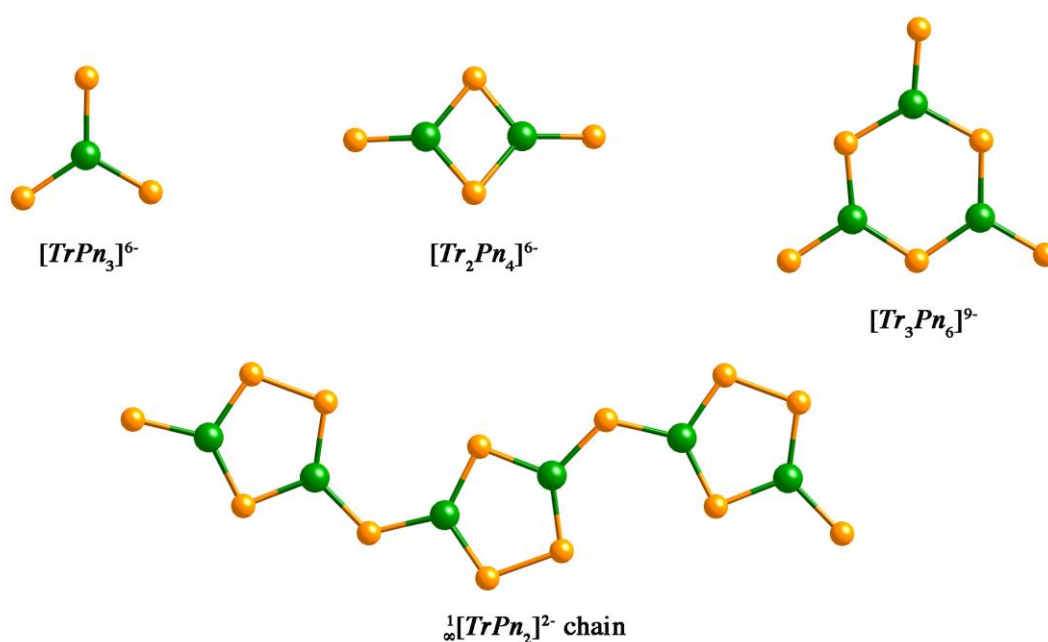
Three-coordinated Ga (or a triel element in general) is much less common within the *A-Tr-Pn* compounds than the four-coordinated tetrahedral geometry, which appears to be the prevailing building block among such solids. Examples of borate-like (or carbonate-like) $[\text{TrPn}_3]^{6-}$ units exist and can be exemplified by $[\text{InAs}_3]^{6-}$ seen in the K_6InAs_3 structure [18]; $[\text{Ga}_2\text{P}_4]^{6-}$ found in the Rb_3GaP_2 structure [16] can be cited as an example of 4-membered rings formed via condensation of two $[\text{GaP}_3]^{6-}$ units into $[\text{Ga}_2\text{P}_4]^{6-}$ dimers (isosteric with 1,3-Dioxetanedione). Higher oligomers, such as the cyclic trimers $[\text{Ga}_3\text{Pn}_6]^{9-}$ that present 6-membered rings are known in the $\text{K}_{20}(\text{Ga}_3\text{Pn}_6)_2\text{Pn}_{0.66}$ structures [12] and in the structures of the title compounds. Since the $[\text{TrPn}_3]^{6-}$ unit is a planar structural motif, it is not common for it to form structures in higher dimension. A search of the ICSD database only reveals the ${}^1_\infty[\text{GaPn}_2]^{2-}$ chain found in the K_2GaP_2 type structure [19]. In this bonding arrangement, 5-membered rings are generated by sharing one common *Pn* and forming one *Pn*–*Pn* bond between every two $[\text{GaPn}_3]^{6-}$ units—these 5-membered rings are further connected to form an infinite chain using the third *Pn* atom as a linker (Figure 2).

Table 1. Important interatomic distances (Å) in $\text{RbNa}_8\text{Ga}_3\text{Pn}_6$ ($\text{Pn} = \text{As}, \text{P}$).

	$\text{RbNa}_8\text{Ga}_3\text{As}_6$	$\text{RbNa}_8\text{Ga}_3\text{P}_6$		$\text{RbNa}_8\text{Ga}_3\text{As}_6$	$\text{RbNa}_8\text{Ga}_3\text{P}_6$
Ga1– $\text{Pn}1$	2.335(1)	2.245(2)	Na3– $\text{Pn}2$	3.015(3)	2.935(3)
$\text{Pn}2$	2.388(1)	2.303(2)	$\text{Pn}3$ ($\times 2$)	3.235(2)	3.158(2)
$\text{Pn}3$	2.400(1)	2.312(2)	$\text{Pn}5$ ($\times 2$)	3.270(2)	3.213(2)
Ga2– $\text{Pn}4$	2.351(1)	2.259(2)	Ga3 ($\times 2$)	3.270(2)	3.216(2)
$\text{Pn}2$	2.383(1)	2.300(2)	Na4– Ga2 ($\times 2$)	3.336(2)	3.260(2)
$\text{Pn}6$	2.391(1)	2.309(2)	Ga3 ($\times 2$)	3.346(2)	3.257(2)
Ga3– $\text{Pn}5$	2.351(1)	2.259(2)	Ga1 ($\times 2$)	3.364(2)	3.282(2)
$\text{Pn}3$	2.418(1)	2.329(2)	$\text{Pn}3$ ($\times 2$)	3.375(2)	3.265(2)
$\text{Pn}6$	2.422(1)	2.337(2)	$\text{Pn}6$ ($\times 2$)	3.416(2)	3.314(2)
$\text{Pn}1$ – Ga1	2.335(1)	2.245(2)	$\text{Pn}2$ ($\times 2$)	3.500(2)	3.401(2)
$\text{Pn}2$ – Ga1	2.388(1)	2.303(2)	Na5– $\text{Pn}3$	2.967(3)	2.892(3)
Ga2	2.383(1)	2.300(2)	$\text{Pn}2$ ($\times 2$)	3.190(2)	3.116(2)
$\text{Pn}3$ – Ga1	2.400(1)	2.312(2)	$\text{Pn}4$ ($\times 2$)	3.338(2)	3.278(2)
Ga3	2.418(1)	2.329(2)	Ga2 ($\times 2$)	3.296(2)	3.244(2)
$\text{Pn}4$ – Ga2	2.351(1)	2.259(2)	Na6– $\text{Pn}4$	2.970(3)	2.882(3)
$\text{Pn}5$ – Ga3	2.351(1)	2.259(2)	$\text{Pn}1$ ($\times 2$)	3.211(2)	3.126(2)
$\text{Pn}6$ – Ga2	2.391(1)	2.309(2)	$\text{Pn}3$ ($\times 2$)	3.386(2)	3.328(2)
Ga3	2.422(1)	2.337(2)	Ga1 ($\times 2$)	3.240(2)	3.181(2)
Rb– $\text{Pn}1$ ($\times 2$)	3.5491(9)	3.487(1)	Na7– $\text{Pn}5$	3.019(3)	2.933(3)
$\text{Pn}6$ ($\times 2$)	3.5929(9)	3.523(1)	$\text{Pn}1$ ($\times 2$)	3.209(2)	3.134(2)
$\text{Pn}5$ ($\times 2$)	3.6975(9)	3.623(1)	$\text{Pn}2$ ($\times 2$)	3.343(2)	3.280(2)
Ga3 ($\times 2$)	3.735(1)	3.6707(8)	Ga1 ($\times 2$)	3.284(2)	3.227(2)
Na1– $\text{Pn}5$ ($\times 2$)	2.992(2)	2.931(2)	Na8– $\text{Pn}4$	2.967(3)	2.874(3)
$\text{Pn}1$	3.018(3)	2.965(3)	$\text{Pn}4$ ($\times 2$)	3.239(2)	3.176(2)
$\text{Pn}5$	3.117(3)	3.051(3)	$\text{Pn}6$ ($\times 2$)	3.330(2)	3.250(2)
Na2– $\text{Pn}4$ ($\times 2$)	2.967(2)	2.909(2)	Ga2 ($\times 2$)	3.245(2)	3.183(2)
$\text{Pn}1$	2.970(3)	2.911(3)			
$\text{Pn}6$	3.069(3)	3.008(3)			

Table 2. Selected angles (°) in $\text{RbNa}_8\text{Ga}_3\text{Pn}_6$ ($\text{Pn} = \text{As}, \text{P}$).

	$\text{RbNa}_8\text{Ga}_3\text{As}_6$	$\text{RbNa}_8\text{Ga}_3\text{P}_6$		$\text{RbNa}_8\text{Ga}_3\text{As}_6$	$\text{RbNa}_8\text{Ga}_3\text{P}_6$
Pn1-Ga1-Pn2	115.89(4)	116.42(7)	Pn5-Ga3-Pn3	113.79(4)	114.48(7)
Pn1-Ga1-Pn3	119.19(4)	119.78(7)	Pn5-Ga3-Pn6	124.65(4)	125.05(7)
Pn2-Ga1-Pn3	124.92(4)	123.81(7)	Pn3-Ga3-Pn6	121.56(4)	120.47(7)
Pn4-Ga2-Pn2	114.31(4)	114.77(7)	Ga2-Pn2-Ga1	113.01(4)	114.04(8)
Pn4-Ga2-Pn6	117.77(4)	118.39(7)	Ga1-Pn3-Ga3	117.57(4)	118.85(8)
Pn2-Ga2-Pn6	127.93(4)	126.84(7)	Ga2-Pn6-Ga3	115.01(4)	115.98(7)

Figure 2. Diverse structural motifs based on the $[\text{TrPn}_3]^{6-}$ unit ($\text{Tr} = \text{triel}, \text{Pn} = \text{pnictogen}$).

As we already mentioned, there are nine crystallographically different cations in the $\text{RbNa}_8\text{Ga}_3\text{Pn}_6$ structure and they have subtly different coordination environments. The large Rb cation is coordinated to six pnictogen atoms that form trigonal prism, with Rb-Pn distances falling in the range from 3.549 to 3.698 Å for Rb-As , and from 3.487 to 3.623 Å for Rb-P (Table 1). Two Ga atoms are found at a little longer distance, enlarging the Rb first coordination sphere to the shape of a quadrilateral prism (Figure 3). Three different local environments could be found for Na: Na1 and Na2 are found in a tetrahedral surrounding of four pnictogen atoms; square pyramids formed by five next-nearest pnictogen atoms are observed for Na3, Na5, Na6, Na7, and Na8—notice that the bases of the square-pyramids are capped by two Ga atoms, enlarging the coordination number to 7; and a hexagonal prism for Na4, where each hexagonal base is formed by three Ga and three Pn atoms. The Na-Pn distances fall into a very wide range due to the different coordination numbers (CN) for Na, with the shortest Na-Pn distance noted for 4-coordinated Na, and the longest Na-Pn distance found for the 12-coordinated Na (Table 1).

Figure 3. Cation coordination in $\text{RbNa}_8\text{Ga}_3\text{Pn}_6$. The polyhedron around Rb is shown in purple (a); Na1 and Na2 in light blue (b); Na3, Na5, Na6, Na7, and Na8 in dark blue (c); and Na4 in olive (d). See text for details.

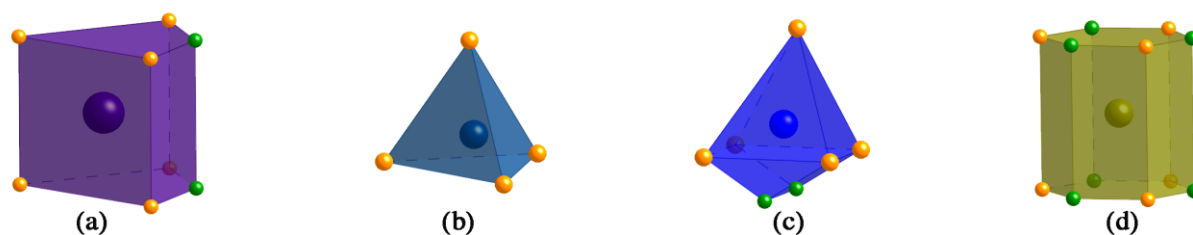
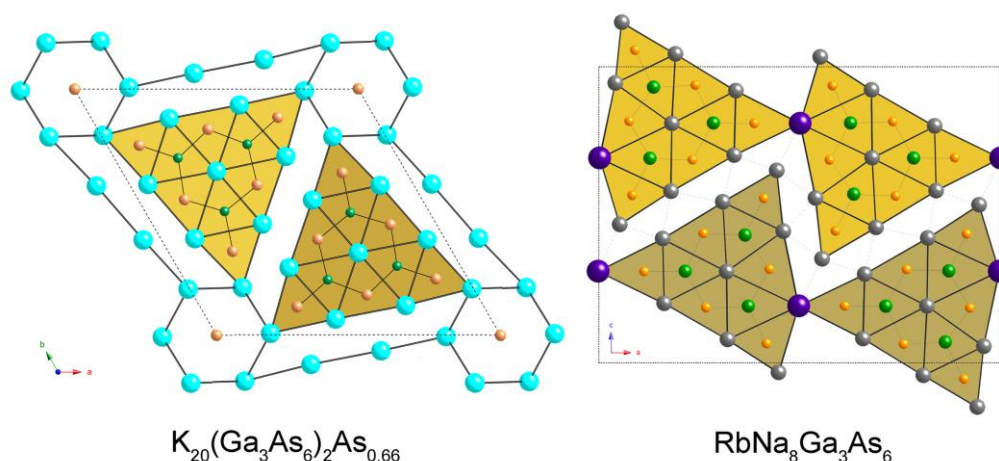


Figure 4. Side-by-side comparison of the cation packing in the crystal structures of $\text{K}_{20}(\text{Ga}_3\text{As}_6)_2\text{As}_{0.66}$ and $\text{RbNa}_8\text{Ga}_3\text{As}_6$, where the trigonal prisms formed by the cations are emphasized. Different shades represent the different heights in the projected directions. The corresponding elements are color-coded as follows: Ga—green; Pn—orange; K—light blue; Rb—purple; and Na—grey. The covalent Ga—As bonds and the unit cells are outlined too.



As already noted, the $[\text{Ga}_3\text{Pn}_6]^{9-}$ 6-membered motif is not without a precedent, having been reported for some time already in $\text{K}_{20}(\text{Ga}_3\text{Pn}_6)_2\text{Pn}_{0.66}$ (defect $\text{Ho}_6\text{Ni}_{20}\text{P}_{13}$ structure type, Pearson symbol $hP39$) [11,12]. However, in the latter hexagonal structure, in addition to the $[\text{Ga}_3\text{Pn}_6]^{9-}$ polyanions, there are isolated Pn^{3-} anions (note the partial occupancy of this site). Apparently, a single cation like K^+ cannot pack well enough with the $[\text{Ga}_3\text{Pn}_6]^{9-}$ polyanions, requiring some subtle rearrangements to accommodate the counterbalancing Pn^{3-} anions. Following the notion of describing the structure from the standpoint of cation packing, in analogy with what has already been presented for $\text{K}_{20}(\text{Ga}_3\text{Pn}_6)_2\text{Pn}_{0.66}$ [12], one can see that the cation arrangements in both cases are actually very similar. From Figure 4, it can be seen that in both structures, apart from the partially occupied Pn atoms in the $\text{K}_{20}(\text{Ga}_3\text{Pn}_6)_2\text{Pn}_{0.66}$ structure, which reside in large hexagonal channels, all Ga and Pn atoms are at the centers of trigonal prisms formed by the cations. Nine such trigonal prisms are conjoined, forming a much larger prism that encloses the entire $[\text{Ga}_3\text{Pn}_6]^{9-}$ unit. The difference is

that in $K_{20}(Ga_3Pn_6)_2Pn_{0.66}$, these larger trigonal prisms can be noted as discrete components, while in $RbNa_8Ga_3Pn_6 (=Rb_2Na_{16}(Ga_3Pn_6)_2)$, *i.e.*, two cations less per formula) they further connect with each other along the a axis by sharing Rb atoms (Figure 4). It seems that the much bigger Rb brings the necessary distortion to the larger trigonal prisms, which leads to a slightly different packing of the cations compared with $K_{20}(Ga_3Pn_6)_2Pn_{0.66}$.

$Na_{10}NbGaAs_6$ crystallizes with the monoclinic space group $P2_1/n$ (No. 14, Pearson symbol $mP36$), and is found to be isoelectronic and isostructural to the Zintl compound $K_{10}NbInAs_6$ [13]. The structure is composed of isolated dimers of edge-shared tetrahedra ($NbAs_4$ or $GaAs_4$), which are isosteric with diborane, B_2H_6 . These dimeric units are separated by the alkali metal cations (Figure 5). Note that there is only one tetrahedral site in the structure, which is co-occupied by Ga and Nb in equal amounts. In the earlier paper on $K_{10}NbInAs_6$, a diamagnetic response from the magnetic susceptibility of the compound can be inferred, suggesting the Nb to be assigned as Nb^{5+} (*i.e.*, d^0 closed-shell species) [13]. This argument allows for the structure to be rationalized readily as $(K^+)_{10}Nb^{5+}In^{3+}(As^{3-})_6$. Clearly, the same approach will be applicable to $Na_{10}NbGaAs_6$ (e.g., $(Na^+)_{10}Nb^{5+}Ga^{3+}(As^{3-})_6$), which means that it can be classified as a Zintl compound with a transition metal [13,20].

Figure 5. (a) Crystal structure of $Na_{10}NbGaAs_6$, viewed along the a axis; (b) representation of $[(As)_2Nb(\mu-As)_2Ga(As)_2]^{10-}$ with thermal ellipsoids, drawn at the 95% probability. The atoms at the centers of the tetrahedra of As atoms are statistically distributed Nb and Ga. The corresponding elements are color-coded as follows: Ga/Nb—light blue; As—orange; and Na—grey.

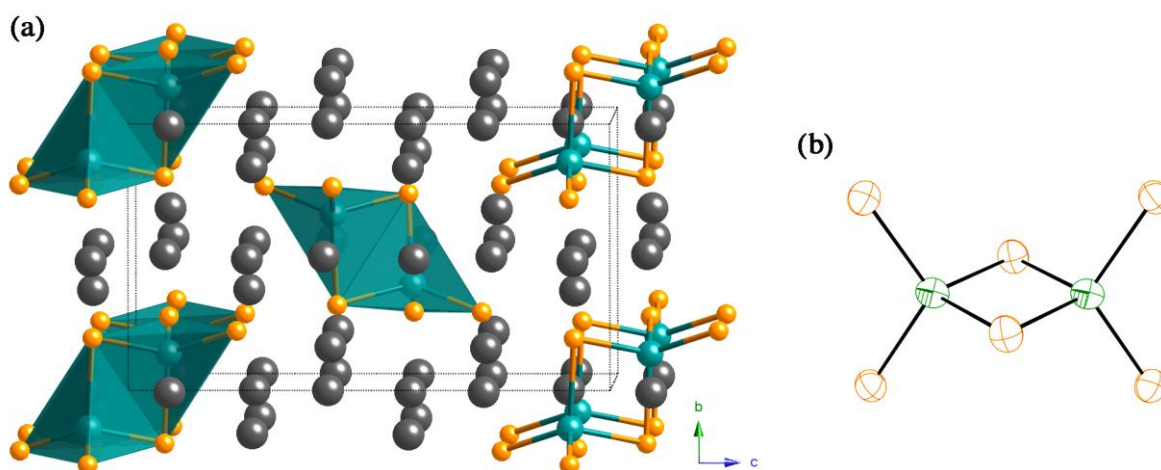


Table 3. Selected interatomic distances (\AA) and angles ($^\circ$) in $Na_{10}NbGaAs_6$.

Nb/Ga–	As3	2.4855(6)	As3-Nb/Ga-As2	114.20(2)
	As2	2.4959(6)	As3-Nb/Ga-As1	108.68(2)
	As1	2.5274(6)	As2-Nb/Ga-As1	113.79(2)
	As1	2.5645(6)	As3-Nb/Ga-As1	111.17(2)
			As2-Nb/Ga-As1	106.78(2)
			As1-Nb/Ga-As1	101.49(2)

The Nb/Ga–As distances fall in the range of 2.4855(6) to 2.5645(6) Å, and all of the As–Nb/Ga–As angles are close to the ideal tetrahedral angle 109°28' (Table 3). An examination of the structures of some compounds with ordered GaAs₄ and NbAs₄ tetrahedra reveals similar lengths for the Ga–As and Nb–As bonds. For example, the Ga–As bonds range from 2.444 to 2.556 Å in K₃Ga₃As₄ [9], and from 2.435 to 2.599 Å in Na₂Ga₂As₃ [21], respectively. The Nb–As distances, as reported for K₃₈Nb₇As₂₄ [22] fall in the range of 2.444–2.571 Å; very similar values for $d_{\text{Nb–As}}$ are seen in Cs₉Nb₂As₆ (2.464–2.592 Å) [22]. Since the established ranges for the Nb–As and Ga–As distances are similar, refinements of the thermal ellipsoids in Na₁₀NbGaAs₆ do not show any abnormal behavior—in fact they are virtually spherical. This is not the case for K₁₀NbInAs₆, where the significant difference between the lengths of the Nb–As and In–As bonds gives rise to characteristic features in their thermal ellipsoids—the thermal ellipsoids of the bridging As atoms are elongated tangentially to the central square (Nb/In–As–Nb/In–As). This observation has been considered as a key evidence of these dimers being heteroatomic [(As)₂Nb(μ -As)₂In(As)₂] species, and not an equimolar mixture of [(As)₂Nb(μ -As)₂Nb(As)₂] and [(As)₂In(μ -As)₂In(As)₂] dimers [13].

3. Experimental Section

All the manipulations involving alkali metals were performed either inside an argon-filled glove box or under vacuum. The starting materials were elemental Rb, Na, Ga, As, and P, either from Alfa Aesar or Aldrich with the stated purity higher than 99.9%. Crystals of RbNa₈Ga₃As₆ were first identified from a reaction starting with Na/Rb/Ga/As with a molar ratio of 16/8/80/56, which was originally attempted for type II clathrate Na₁₆Rb₈Ga₈₀As₅₆. The elements with a total mass of ca. 500 mg were loaded into a niobium ampoule, which was subsequently arc-welded under high purity Ar and then jacketed in a fused silica tube under vacuum. The reaction mixture was heated up to 550 °C, and equilibrated for one week before it was slowly cooled to room temperature. This experiment resulted in black, small crystals of RbNa₈Ga₃As₆, which were found to be extremely air-sensitive and had to be handled with great care. After the composition was established, the reaction was repeated with the correct stoichiometry. However, besides RbNa₈Ga₃As₆, Na₁₀NbGaAs₆, which formed from a side reaction with the Nb container, was also identified. This observation indicated that Nb containers were not well suited for such reactions; more expensive Ta or Mo tubes should be considered. RbNa₈Ga₃P₆ could be synthesized from the same setup as well as the same heat treatment, with the coexistence of another known Zintl compound, Na₆GaP₃ [23].

The crystal structures of the title compounds were established using single-crystal X-ray diffraction with a Bruker SMART CCD-based diffractometer (monochromated Mo K α_1 radiation). Crystals with suitable dimensions (<100 μm) were mounted on glass fiber with Paratone-N oil, and then quickly transferred to the goniometer of the diffractometer. A cold nitrogen stream (200(2) K) was used to keep the crystals at low temperature as well as to protect them from being oxidized. Full spheres of data were collected in four batch runs with a frame width of 0.4° for ω and θ . Integration of the intensity data was done with the SAINT program [24], and semi-empirical absorption correction based on equivalents was applied with the SADABS code [25]. The structures were solved by direct method and refined to convergence by full matrix least squares on F^2 using the SHELXTL package [26]. The unit

cell axes and the atomic coordinates of $\text{RbNa}_8\text{Ga}_3\text{Pn}_6$ were standardized with the aid of the Structure TIDY [27] in the last refinement cycles.

The structure refinements for $\text{Na}_{10}\text{NbGaAs}_6$ required some specific attention. In this structure, the tetrahedrally coordinated site was originally assigned as Ga, which is a common coordination environment for it. However, the thermal displacement parameter in this situation was unreasonably small. Based on the discussion on $\text{K}_{10}\text{NbInAs}_6$ structure, the model that this site was co-occupied by Ga and Nb was considered, where Nb was from the reaction vessel. Such refinement lead to nearly half and half occupancy of Ga and Nb, *i.e.*, 49% Ga and 51% Nb. Thus, the ratio was fixed at 1:1 in the final refinement cycle, which resulted in R_1 values as low as 0.0263 and reasonable thermal ellipsoids.

Selected crystal data and refinement parameters are given in Table 4; important bond distances and angles are listed in Tables 1–3. CIFs have also been deposited with the Fachinformationszentrum Karlsruhe, 76344 Eggenstein-Leopoldshafen, Germany, (fax: (49) 7247-808-666; E-Mail: crysdata@fiz.karlsruhe.de)—depository numbers CSD-423946 for $\text{RbNa}_8\text{Ga}_3\text{As}_6$, CSD-423947 for $\text{RbNa}_8\text{Ga}_3\text{P}_6$, and CSD-423948 for $\text{Na}_{10}\text{NbGaAs}_6$.

Table 4. Selected crystal data and structure refinement parameters for $\text{RbNa}_8\text{Ga}_3\text{Pn}_6$ ($\text{Pn} = \text{As}, \text{P}$) and $\text{Na}_{10}\text{NbGaAs}_6$.

Empirical formula		$\text{RbNa}_8\text{Ga}_3\text{As}_6$	$\text{RbNa}_8\text{Ga}_3\text{P}_6$	$\text{Na}_{10}\text{NbGaAs}_6$
Formula weight		928.07	664.37	842.05
Space group, Z		$Pnma$ (No. 62), 4	$Pnma$ (No. 62), 4	$P2_1/n$ (No. 14), 2
Temperature		200(2) K		
Wavelength		Mo $K\alpha$, 0.71073 Å		
Cell parameters	a (Å)	22.843(6)	22.276(3)	8.3243(7)
	b (Å)	4.7892(12)	4.6947(6)	7.5173(6)
	c (Å)	16.861(4)	16.356(2)	13.546(2)
	β (°)			90.908(1)°
	V (Å ³)	1844.6(8)	1710.4(4)	847.58(12)
Calculated density (g/cm ³)		3.342	2.580	3.299
Absorption coefficient (cm ⁻¹)		178.14	82.52	141.13
Crystal size (mm ³)		0.070 × 0.030 × 0.025	0.050 × 0.030 × 0.030	0.060 × 0.055 × 0.035
Reflections collected/independent		24813/2575	22860/2382	10644/1948
R_{int}		0.0888	0.0954	0.0528
Goodness-of-fit on F^2		1.031	1.104	1.006
R_1 ($I > 2\sigma_I$) ^a		0.0326	0.0410	0.0263
wR_2 ($I > 2\sigma_I$) ^a		0.0521	0.0625	0.0464
Largest diff. peak/hole (e ⁻ /Å ³)		1.164/−0.928	0.802/−0.880	0.751/−0.578
Weight coefficient, A/B ^a		0.0163/0	0.0109/1.1965	0.0176/0

^a $R_1 = \sum ||F_o| - |F_c|| / \sum |F_o|$, $wR_2 = \{\sum [w(F_o^2 - F_c^2)^2] / \sum [w(F_o^2)^2]\}^{1/2}$, where $w = 1/[\sigma^2 F_o^2 + (AP)^2 + BP]$, and $P = (F_o^2 + 2F_c^2)/3$. A and B are weight coefficients.

4. Conclusions

Quaternary compounds $\text{RbNa}_8\text{Ga}_3\text{Pn}_6$ ($\text{Pn} = \text{P}, \text{As}$) and $\text{Na}_{10}\text{NbGaAs}_6$ have been synthesized and characterized. These findings suggest that although many ternary compounds of the alkali and alkaline-earth metals with the triels and the pnictogen elements have already been discovered, still little is known about the corresponding systems with two types of cations. Such seemingly trivial approaches can be the key for the synthesis of many more new compounds with novel structures.

Acknowledgments

Svilen Bobev acknowledges financial support from the US Department of Energy through a grant (DE-SC0001360).

References

1. Blake, N.P.; Mollnitz, L.; Kresse, G.; Metiu, H. Why Clathrates are Good Thermoelectrics: A Theoretical Study of $\text{Sr}_8\text{Ga}_{16}\text{Ge}_{30}$. *J. Chem. Phys.* **1999**, *111*, 3133–3144.
2. Kuznetsov, V.L.; Kuznetsova, L.A.; Kaliazin, A.E.; Rowe, D.M. Preparation and Thermoelectric Properties of $\text{A}_8^{\text{II}}\text{B}_{16}^{\text{III}}\text{B}_{30}^{\text{IV}}$ Clathrate Compounds. *J. Appl. Phys.* **2000**, *87*, 7871–7875.
3. Sales, B.C.; Chakoumakos, B.C.; Jin, R.; Thompson, J.R.; Mandrus, D. Structural, Magnetic, Thermal, and Transport Properties of $\text{X}_8\text{Ga}_{16}\text{Ge}_{30}$ ($\text{X} = \text{Eu}, \text{Sr}, \text{Ba}$) Single Crystals. *Phys. Rev. B* **2001**, *63*, 245113.
4. Saramat, A.; Svensson, G.; Palmqvist, A.E.C.; Stiewe, C.; Mueller, E.; Platzek, D.; Williams, S.G.K.; Rowe, D.M.; Bryan, J.D.; Stucky, G.D. Large Thermoelectric Figure of Merit at High Temperature in Czochralski-Grown Clathrate $\text{Ba}_8\text{Ga}_{16}\text{Ge}_{30}$. *J. Appl. Phys.* **2006**, *99*, 023708.
5. Bobev, S.; Meyers, J., Jr.; Fritsch, V.; Yamasaki, Y. Synthesis and Structural Characterization of Novel Clathrate-II Compounds of Silicon. In *Proceedings of 25th International Conference on Thermoelectrics 2006 (ICT'06)*, Vienna, Austria, 6–10 August 2006; IEEE: New York, NY, USA, 2006; Volume 25, pp. 48–52.
6. He, H.; Tyson, C.; Bobev, S. University of Delaware, Newark, DE 19716, USA. Unpublished Results. 2012.
7. Cordier, G.; Ochmann, H. Na_3AlAs_2 , a Zintl Phase with SiS_2 -Isosteric Anions. *Z. Naturforsch.* **1988**, *43*, 1538–1540.
8. Cordier, G.; Ochmann, H.; Schaefer, H. New Types of Al_2As_3 -Chains in $\text{K}_3\text{Al}_2\text{As}_3$. *Rev. Chim. Miner.* **1985**, *22*, 58–63.
9. Cordier, G.; Ochmann, H.; Schaefer, H. $\text{Na}_2\text{Al}_2\text{Sb}_3$ and $\text{K}_2\text{Al}_2\text{Sb}_3$, Two New Zintl Phases with Layered Anions. *Rev. Chim. Miner.* **1984**, *21*, 282–291.
10. Birdwhistell, T.L.T.; Stevens, E.D.; O'Connor, C.J. Synthesis and Crystal Structure of a Novel Layered Zintl Phase: $\text{K}_3\text{Ga}_3\text{As}_4$. *Inorg. Chem.* **1990**, *29*, 3892–3894.
11. Bobev, S.; Sevov, S.C. Five Ternary Zintl Phases in the Systems Alkali-Metal-Indium-Bismuth. *J. Solid State Chem.* **2001**, *163*, 436–448.
12. Cordier, G.; Ochmann, H. $\text{K}_{20}\text{Ga}_6\text{Sb}_{12.66}$ and $\text{K}_{20}\text{Ga}_6\text{As}_{12.66}$, Compounds with $(\text{Ga}_3\text{Sb}_6)^{9-}$ Anion and $(\text{Ga}_3\text{As}_6)^{9-}$ Anion Isostructural to $(\text{B}_3\text{O}_6)^{3-}$. *Z. Naturforsch.* **1990**, *45*, 277–282.

13. Gascoin, F.; Sevov, S.C. Synthesis and Characterization of Transition Metal Zintl phases: $K_{10}NbInAs_6$ and $K_9Nb_2As_6$. *Inorg. Chem.* **2003**, *42*, 904–907.
14. Pauling, L. *The Nature of the Chemical Bond*, 3rd ed.; Cornell University Press: Ithaca, NY, USA, 1960; pp. 400–404.
15. Cordier, G.; Ochmann, H. Crystal Structure of Dirubidium Catena-Diarsenidogallate, Rb_2GaAs_2 . *Z. Kristallogr.* **1991**, *195*, 113–114.
16. Somer, M.; Peters, K.; Thiery, D.; von Schnering, H.G. Crystal Structure of Trirubidium Diphosphidogallate, Rb_3GaP_2 . *Z. Kristallogr.* **1990**, *192*, 271–272.
17. Zintl, E. Internietallische Verbindungen. *Angew. Chem.* **1939**, *52*, 1–6.
18. Blase, W.; Cordier, G.; Somer, M. Crystal Structure of Hexapotassium Triarsenidoindate, K_6InAs_3 . *Z. Kristallogr.* **1993**, *206*, 141–142.
19. Blase, W.; Cordier, G.; Somer, M. Crystal Structure of Dipotassium Catena-Diphosphidogallate, K_2GaP_2 . *Z. Kristallogr.* **1991**, *195*, 115–116.
20. Kauzlarich, S.M. Transition Metal Zintl Compounds. In *Chemistry, Structure, and Bonding of Zintl Phases and Ions*; Kauzlarich, S.M., Ed.; VCH: New York, NY, USA, 1996; pp. 245–274.
21. Cordier, G.; Ochmann, H. Crystal Structure of Disodium Phyllo-triarsenidodigallate, $Na_2Ga_2As_3$. *Z. Kristallogr.* **1991**, *197*, 285–286.
22. Gascoin, F.; Sevov, S.C. Synthesis and Characterization of $K_{38}Nb_7As_{24}$ and $Cs_9Nb_2As_6$. *Inorg. Chem.* **2002**, *41*, 5920–5924.
23. Blase, W.; Cordier, G.; Somer, M. Crystal Structure of Hexasodium Triphosphidogallate, Na_6GaP_3 . *Z. Kristallogr.* **1993**, *206*, 143–144.
24. *SMART & SAINT*; Bruker Analytical X-ray Systems, Inc.: Madison, WI, USA, 2003.
25. Sheldrick, G.M. *SADABS*; University of Göttingen: Göttingen, Germany, 2003.
26. Sheldrick, G.M. *SHELXTL*; University of Göttingen: Göttingen, Germany, 2001.
27. Gelato, L.M.; Parthe, E. Structure Tidy—a Computer Program to Standardize Crystal Structure Data. *J. Appl. Crystallogr.* **1987**, *20*, 139–146.